*Article*

# Production, Activation and $CO_2$ Uptake Capacity of a Carbonaceous Microporous Material from Palm Oil Residues

Cristina Moliner [1], Simona Focacci [1], Beatrice Antonucci [1], Aldo Moreno [2], Simba Biti [2], Fazlena Hamzah [3], Alfonso Martinez-Felipe [2,4], Elisabetta Arato [1,*] and Claudia Fernández Martín [2,4]

[1]   Department of Civil, Chemical and Environmental Engineering, University of Genoa, Via Opera Pia 15, 16145 Genoa, Italy
[2]   Chemical Process and Materials Research Group, School of Engineering, King's College, University of Aberdeen, Aberdeen AB24 3UE, UK
[3]   School of Chemical Engineering, College of Engineering, Universiti Teknologi MARA, Shah Alam 40450, Selangor, Malaysia
[4]   Centre for Energy Transition, King's College, University of Aberdeen, Aberdeen AB24 3UE, UK
*   Correspondence: elisabetta.arato@unige.it

**Abstract:** While Malaysia produces about half of the world's palm oil and is the largest producer and exporter worldwide, oil palm industries generate large amounts of lignocellulosic biomass waste as a sub-product with no economic market value other than feedstock for energy valorisation. With the aim to increase the sustainability of the sector, in this work we prepare new materials for $CO_2$ capture from palm oil residues (empty fruit bunches and kernels). The biochar is obtained through the carbonisation of the residues and is physically and chemically activated to produce porous materials. The resulting microporous samples have similar properties to other commercial activated carbons, with BET surfaces in the 320–880 $m^2$/g range and pore volumes of 0.1–0.3 $cm^3 \cdot g^{-1}$. The $CO_2$ uptake at room temperature for physically activated biochar (AC) was 2.4–3.6 $mmolCO_2$/gAC, whereas the average $CO_2$ uptake for chemically activated biochar was 3.36–3.80 $mmolCO_2$/gAC. The amount of $CO_2$ adsorbed decreased at the highest temperature, as expected due to the exothermic nature of adsorption. These findings confirm the high potential of palm oil tree residues as sustainable materials for $CO_2$ capture.

**Keywords:** palm oil waste; $CO_2$ uptake; adsorption; chemical and physical activation; biochar

## 1. Introduction

Over 76 million tons of palm oil were produced worldwide in 2020 [1], of which 40% were solid wastes. As a result, the palm oil industry generates one of the most abundant biomass residues with a generation of circa 30 million tons. Malaysia dedicates 45.2% of its total land plantation to palm oil and is the world's largest producer and exporter, contributing to about half of the total production [2,3]. Oil palm industries produce, together with oil palm as the main product, a great quantity of lignocellulosic biomass, considered as waste, including oil palm trunks (OPT), oil palm fronds (OPF), empty fruit bunches (EFB), palm oil fibres (POF), palm kernel shells (PKS) and palm oil mill effluent palm (POME). These large-scale industrial activities generate large amounts of waste with low or no economic value other than, in some cases, energy generation. Such disposal emergency has been recently aggravated after the Department of Environment in Malaysia banned open burning [4].

In addition to waste generation, the palm oil industry is responsible for a high amount of Greenhouse Gases (GHGs) that are generated at various stages (transportation of raw material, combustion of fuel in boilers or main oil production steps) [5]. Carbon, Capture and Storage (CCS) continues to develop as a central strategy to mitigate GHGs emissions.

The main existing CCS technologies include adsorption using activated carbons (ACs), zeolites, and new materials such as metal−organic frameworks (MOFs), polymers, and metal oxides, designed to improve $CO_2$ adsorption efficiencies [6]. ACs are promising adsorbents for carbon capture due to their (i) abundant availability; (ii) low-cost and sustainability; (iii) high surface area and (iv) high adsorptive and high selectivity characteristics tailored by the number and size of pores generated during the activation process. The adsorptive capacity of ACs is induced when the structure of the raw biomass is modified by dehydration and carbonisation, followed by a chemical or physical activation step [7]. These preparation steps define the morphology of the ACs (i.e., surface area, micropore volume and size) which ultimately determines $CO_2$ uptake [8]. Khandaker et al. [8] stated that the control of micropores had greater importance for adsorbing high $CO_2$ compared to surface area and total pore volume and Deng et al. [9] reported that a pore size of 0.33–0.63 nm played an important role in maximizing the $CO_2$ uptake. It is also noteworthy, in any case, that temperature and pressure also affect gas adsorption to a great extent.

Production of activated carbon (AC) from agricultural byproducts has gained increased interest in recent years because of their abundance, high carbon content and cheap availability. Many agricultural residues have been tested as AC precursors, such as wheat, corn straw, olive stones, bagasse, birch wood, sunflower shell, almond shells, peach stones, straw, or rice husks, among others [10]. The production of ACs usually involves a first carbonisation step followed by an activation method: physical activation, with carbon dioxide, steam, or air at elevated temperatures [11], and chemical activation with chemical activating agents, such as dehydrating agents and oxidants. The most common chemical agents are $ZnCl_2$, KOH, $H_3PO_4$ or $K_2CO_3$ [12]. The selection of the activation method will result in different physicochemical properties of the activated carbon, such as surface area, micropore and mesopore distribution, total pore volume or surface functionality, which will define their adequacy and efficiency as adsorbent materials.

Several activated carbons obtained from agricultural waste have been postulated for $CO_2$ adsorption in pure and mixed streams, [13,14] and more specifically, palm oil residues have been used in gas and water treatment. Promraksa et al., for example, pyrolyzed PKS, EFB and POF obtaining a biochar with 0.46 mmol/g capacity for $CO_2$ adsorption [15]. Ibrahim et al. carbonised oil palm biomass, which was further functionalized with nitric acid, facilitating the adsorption of various pollutants from aqueous solutions, such as dyes and heavy metals [16]. Lawal et al. produced activated biochar from palm oil biomass that was then used for water treatment in the palm oil effluents, making the wastewater suitable for reuse in palm oil mills and safe for discharge into the aquatic environment [17]. The same authors also predicted uptake yields and selectivity at varying conditions through molecular dynamic simulations [18].

In this work, we report the preparation and activation of carbons from palm oil residues (Section 3) that have been then used as $CO_2$ adsorbents for an equimolar mixture of $CO_2/N_2$. To do so, we have designed and assembled an experimental set-up to obtain breakthrough curves of $CO_2$ uptake in carbon-based materials (Section 3). In Section 3, we discuss our results and compare them with other adsorbent materials in terms of suitability and efficiency. The outcomes highlight that our strategy can be a sustainable alternative to the disposal and open-burning of palm oil residues, simultaneously giving added value to residues, and ultimately promoting circular economies.

## 2. Materials and Methods

### 2.1. Materials

Palm oil residues (empty fruit bunches and kernels, Figure 1a) were obtained from Paloh Oil Palm Mill, Kelantan, Malaysia. Samples were first washed in distilled water several times and then dried in an oven at 100 °C for one day to remove moisture. After drying, samples were manually crushed in a mortar and sieved to obtain particles with diameters between 1.5 mm and 3.5 mm. The resulting feedstock was stored for further use and analyses (Figure 1b). A 0.5M sodium hydroxide solution was prepared from solid

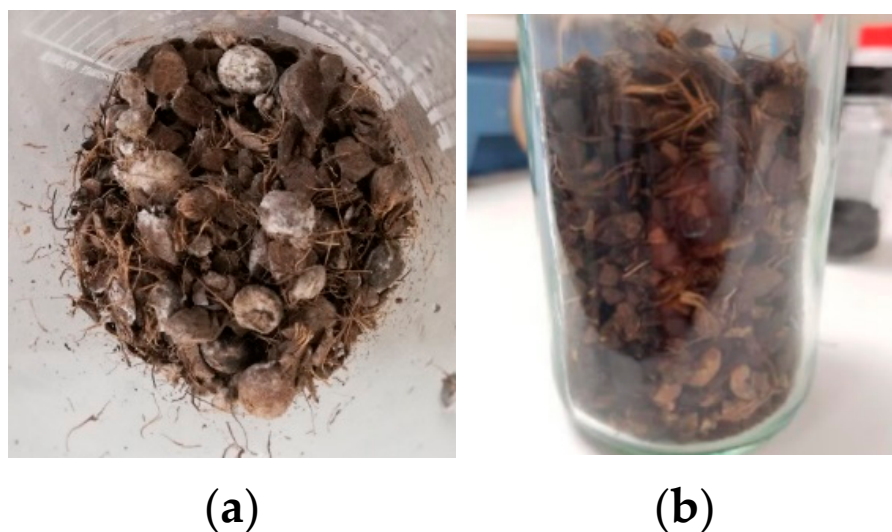granules (Acrōs Organics®, Geelm Belgium) and used for the chemical activation step (see Section 2.3).



**Figure 1.** Palm oil residues, POR, as received (**a**) and after pre-treatment (**b**).

## 2.2. Preparation of Porous Carbons

Figure 2 shows the bench scale experimental set-up employed for carbonisation. Samples were prepared in a purpose-designed quartz reactor sat within a Nabertherm tubular furnace (RT 50-250/11). The quartz reactor was connected to a flow-controlled $N_2$ stream (in the range of 0–250 mL·min$^{-1}$), controlled through a gas flowmeter (Omega®, Aberdeen, UK). The exit gas went through a Drechsel glass bottle filled with cold water, where the produced bio-oil was trapped. The part of the vessel that remained outside the furnace was covered with an insulating material to avoid heat loss.
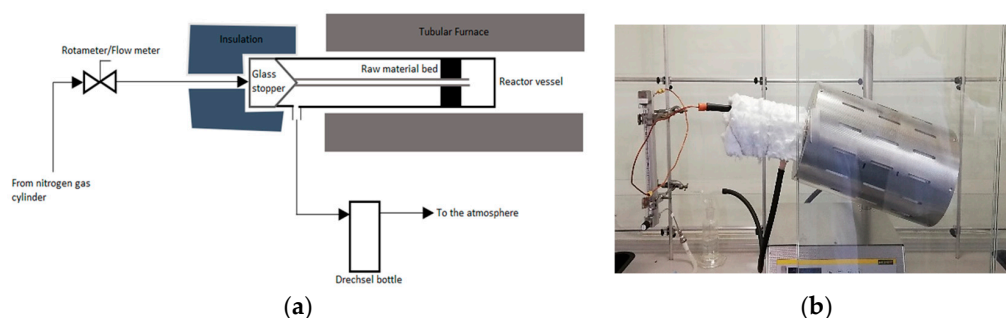


**Figure 2.** Experimental set-up for carbon-based materials synthesis (**a**) and electric tubular furnace containing the quartz vessel (**b**).

Samples were initially weighed (20 ± 0.1 g) and heated in an electric tubular furnace at around 100 °C for 30 min to remove moisture and were further heated at a rate of 10 °C·min$^{-1}$ to the carbonisation temperature, 650 °C, which was held for an hour. The set-up was then allowed to cool down to room temperature to avoid thermal shock and finally, the carbonised sample was removed. The carbon-based material was weighed again to evaluate the initial burn-off percentage (*B*, %) promoted by carbonisation and calculated as [19]:

$$B(\%) = \frac{m_0 - m_f}{m_0} 100 \qquad , \qquad (1)$$

with $m_0$ and $m_f$ the initial and final mass of the samples, respectively.

### 2.3. Carbon Activation Procedure

Activated carbons were prepared via either physical or chemical activation in the same electric furnace used for carbonisation, see Figure 3. An additional inner vessel, namely the activation vessel, was inserted into the external vessel's top hole. The activation vessel's top hole was closed using a rubber stopper, and the outlet gas was directed to a bottle with cold water before being exited into the atmosphere.
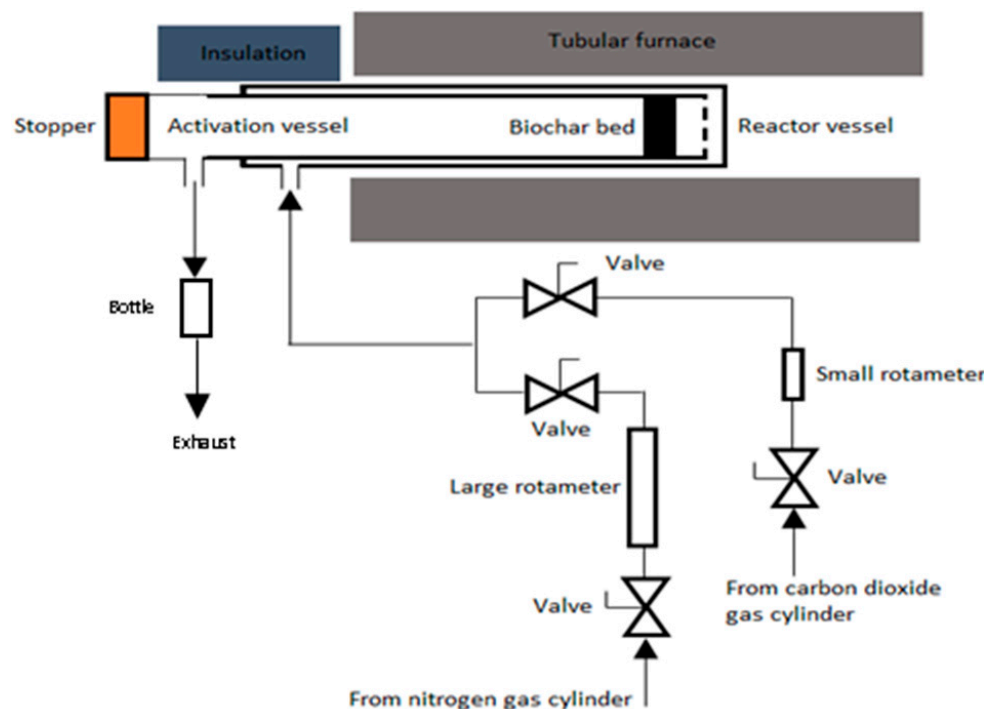


**Figure 3.** Experimental set-up for carbon-based materials physical activation.

Physical activation was carried out using $CO_2$ as an activating agent using a flow equal to 12 mL·min$^{-1}$. The system was heated at a rate of 10 °C·min$^{-1}$ from 100 °C to 900 °C, and the temperature was then maintained for the duration of different times (390–1130 min) to yield a series of activated carbon with various degrees of burn-off. Sodium hydroxide (NaOH 0.5M) was used as the chemical activating agent at different wet impregnation ratios (1:1, 1:2 and 1:3) with respect to the carbonous substrate. The impregnated samples were heated at 700 °C, held for an hour and then left overnight at room temperature while stirring, to remove the residual NaOH [20,21]. Samples were then cleaned with distilled water, filtered, dried in an oven at 100 °C overnight and weighed.

The resulting activated carbon samples were labelled as POR-AC, where A and S refer to the type of activation (P, physical and C, chemical) and settings (burn-off percentage for physical activation and C:NaOH ratio for chemical activation). For example, POR-C11 will be a palm oil residue activated chemically with a ratio C:NaOH equal to 1:1.

The surface area and porosity of all activated carbons were calculated from the $N_2$ adsorption–desorption isotherms measured at −196 °C with a Micrometrics TriStar 3000 analyser. The specific surface area ($S_{BET}$) was estimated by using the Brunauer–Emmet–Teller (BET) equation. The total pore volume was calculated using Gurvich's law. The Horvath–Kawazoe (HK) method was used to calculate the micropore size distribution. Following the IUPAC classification, pore sizes of 2 and 50 nm represent the boundary of micropores–mesopores and mesopores–macropores, respectively.

### 2.4. $CO_2$ Uptake

All the $CO_2/N_2$ adsorption experiments were carried out in a home-made system at the School of Engineering (University of Aberdeen, Scotland), shown schematically in

Figure 4. The set-up consisted of the following elements: $CO_2$ (UN1013, Linde®, Aberdeen, UK) and $N_2$ (UN1066-OFN of Linde®) pressure bottles; $CO_2$ and $N_2$ manual flowmeters (Omega®); pressure transducer (Omega®) connected to one computer; brass adsorption cell; digital flowmeter (Agilent Technologies®, Cheadle, UK) and $CO_2$ analyzer (G110 Geotech®, Aberdeen, UK).
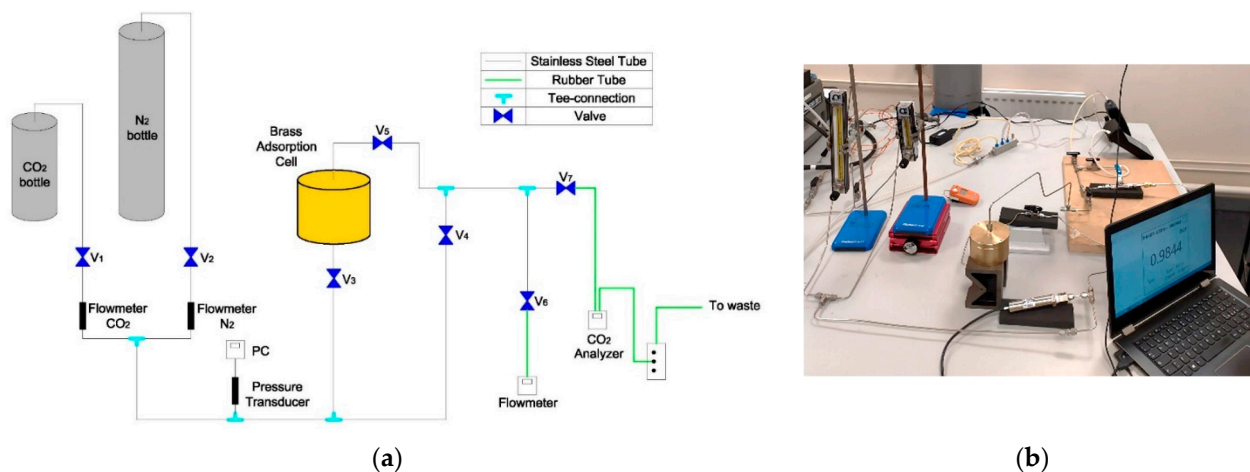


(**a**)                                                    (**b**)

**Figure 4.** Graphical flow diagram of the experimental system (**a**) and lab adsorption system (**b**) (operating at room temperature).

A gas adsorption cell was designed and built to carry out both adsorption and permeability tests, with one or two outputs, respectively (Figure 5a). The gas went through the cell from the bottom side and passed through the sample holder (Figure 5b) where the carbonaceous material under test was placed. The bottom side had a second outlet for the collection of retentate when necessary (and was closed and sealed for adsorption tests to avoid leaks). The cell was covered with rock wool to avoid heat dissipation (Figure 5b).
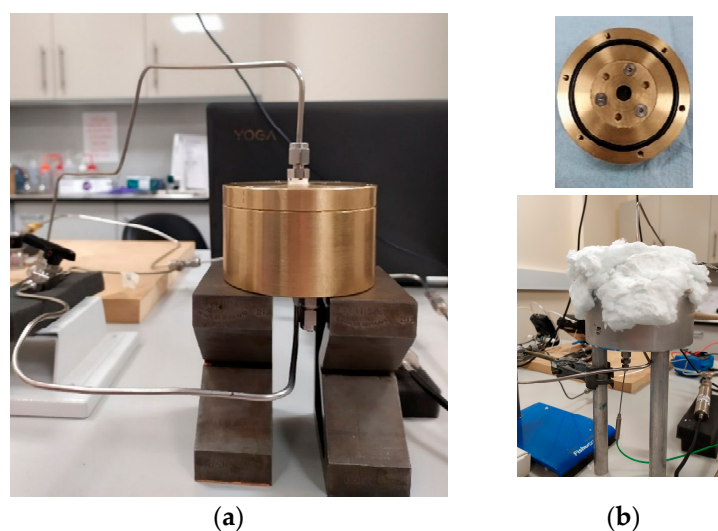


(**a**)                                                    (**b**)

**Figure 5.** Gas adsorption brass cell (**a**) and sampler holder/isolation of the cell (**b**).

Activated carbons obtained as described previously were pelletised using ashes from palm oil as the binding agent, in a mass ratio of 3:2. Corresponding amounts of ACs and ashes (around 0.25 g of ACs and 0.17 g of ashes) were ground in a mortar and two droplets of distilled water were added to create a paste that was placed inside a pellet die set (Figure 6a). The resulting pellets (diameter of 16 mm, Figure 6b) were then obtained using a mould by pressuring at 100 bar for 1 min.
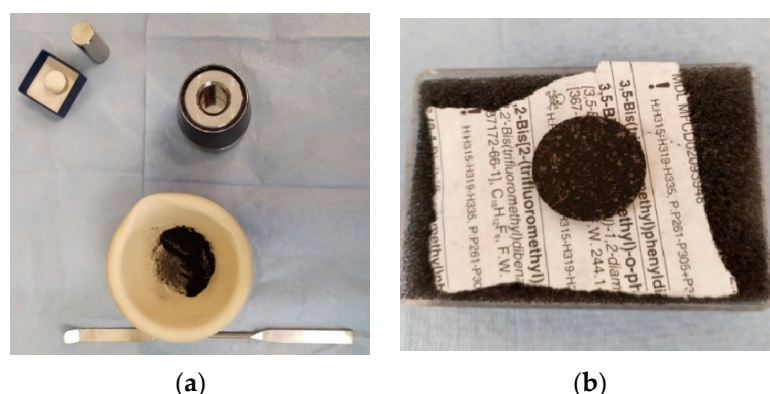
|        (a)        |        (b)        |

**Figure 6.** Pellets (16 mm diameter) die set and sample paste (**a**) and produced pellet (**b**).

The feed gas for the $CO_2$ uptake tests was an equimolar mixture of nitrogen and carbon dioxide at a total flow rate of 100 mL·min$^{-1}$. All the $CO_2$ breakthrough curves were obtained at atmospheric pressure and varying temperatures (25 °C, 125 °C and 225 °C). An electrical heater (Omega$^{®}$) and a Taisuo$^{®}$ temperature controller (STP-321, Nigbo, China) with a thermocouple type J were introduced in the system for tests at higher temperatures.

## 3. Results and Discussion

### 3.1. Production and Characterisation of Activated Carbons

Initially, 20 g of the pre-treated palm oil residues were carbonised following the procedure described in Section 2.1. An average of 70% (weight %) of the initial mass was removed during carbonisation in all samples. The remaining 30% (wt.) of the carbon-based materials was physically or chemically activated, resulting in the samples described in the following paragraphs.

### 3.1.1. Physical Activation

Physical activation of the carbonised samples (~2.5 g) was carried out using $CO_2$. Different burn-off percentages were reached after multiple activation cycles (Table 1), with the total time shown as the sum of the duration of each individual cycle. As shown in the table, the longer the activation time, the further development of $S_{BET}$ and $V_{TOTAL}$ is found. Hence, ACs with higher burn-off showed increased $CO_2$ uptakes compared with their analogous half-burn-off values (20% vs. 40%).

**Table 1.** Physically activated samples.

| Sample | Activation Time (min) | Burn-Off (%) |
|--------|----------------------|--------------|
| POR-P20 | 390 | 23.13 |
| POR-P40 | 1130 | 39.57 |

### 3.1.2. Chemical Activation

Chemical activation of carbonised samples (~1.5 g) was carried out using NaOH, as described in Section 2. The resulting burn-off percentages are gathered in Table 2.

**Table 2.** Chemically activated samples.

| Sample | C:NaOH Mass Ratio | Burn-off (-) |
|--------|-------------------|--------------|
| POR-C11 | 1:1 | 4.34 |
| POR-C12 | 1:2 | 4.90 |
| POR-C13 | 1:3 | 3.39 |

The average pore diameter, surface area and total pore volume of all the ACs were obtained from the isotherms, as described above, and the main results are shown in Table 3. A representative example of N2-adsorption curves is reported in Appendix A.

**Table 3.** BET results for all the produced ACs (correlation coefficient = 0.99) [1].

| Sample | Average Pore Diameter, $d_p$ (nm) * | BET Surface Area, $S_{BET}$ ($m^2 \cdot g^{-1}$) ** | Total Pore Volume, $V_{TOTAL}$ ($cm^3 \cdot g^{-1}$) *** |
|---|---|---|---|
| POR-P20 | 0.67 | 653.5 | 0.22 |
| POR-P40 | 0.68 | 881.5 | 0.30 |
| POR-C11 | 0.80 | 319.0 | 0.11 |
| POR-C12 | 0.77 | 356.0 | 0.22 |

[1] POR-C13 not available, * average error: 0.01 nm, ** average error: 32 $m^2 \cdot g^{-1}$, *** average error: 0.031 $cm^3 \cdot g^{-1}$.

Table 4 gathers the average $CO_2$ uptake for both physically and chemically activated samples at 25 °C. The increasing activation time in the physically activated biochars (higher burn-off percentages) resulted in an increase in the adsorption capacity. This is due to the further developed textural properties (i.e., $S_{BET}$, $V_{Total}$, see Table 3) exhibited by the activated carbons with higher burn-off values. Even though chemical activation was carried out in a single heating step (with lower burn-off percentages), the corresponding ACs had higher adsorption capacity [6] than that showed by the physically activated ones. It is worth noting that the samples with higher NaOH impregnation ratios also show a slightly higher $CO_2$ uptake. This is consistent with the higher surface areas and lower average pore diameters promoted at higher NaOH percentages.

Moreover, especially if the subsequent activation process is carried out at high temperatures and for long periods of time, with greater activation times, the adsorption capacity of the activated carbon increases, obtaining good adsorption results even with samples carbonised at low temperatures [22,23]. It can be deduced then that the process that distinguishes the adsorption capacity of ACs is the activation step, with $CO_2$ uptake values independent of the carbonisation process. Remarkably, previous studies on palm empty fruit bunch showed similar $CO_2$ uptake values compared with this work [24–26]. Commercial AC is also included in the table for comparison.

**Table 4.** $CO_2$ uptake results of the physical and chemical activated samples tested at 25 °C.

| Sample | $CO_2$ Uptake (mmol/g) |
|---|---|
| POR-P20 | 2.41 |
| POR-P40 | 3.58 |
| POR-C11 | 3.36 |
| POR-C12 | 3.75 |
| POR-C13 | 3.81 |
| Commercial AC [27] | 3.84 |

*3.2. Influence of Temperature on $CO_2$ Uptake*

Table 5 gathers the $CO_2$ uptake associated with the breakthrough curves of the two samples with the best performance (chemically activated at ratio 1:2 and 1:3) at two temperatures (125 °C–225 °C). The amount of $CO_2$ adsorbed decreased at the highest temperature, as expected due to the exothermic nature of adsorption (favoured at low temperatures). Interestingly, at higher temperatures, samples with the lowest impregnation ratio performed better, as also observed in other works [28].

The average $CO_2$ uptake value obtained for physically activated carbons in this work was 3.1 mmol$CO_2$/gAC and the average $CO_2$ uptake value for chemically activated carbons was 3.6 mmol$CO_2$/gAC. Figure 7 shows a comparison of the $CO_2$ uptakes obtained in this study with other porous carbons reported in the literature. The capacities of $CO_2$ uptake of our materials are among the best performing in carbon-based adsorbents, studied

under similar operating conditions. It is important to highlight that the key advantages of AC materials are their low cost, their insensitivity to moisture and the possibility of their production/synthesis from numerous carbon-based naturally existing or spent materials.

**Table 5.** $CO_2$ uptake results of the samples tested at 125 °C and 225 °C.

| Sample | $CO_2$ Uptake (mmol/g) | |
|---|---|---|
| | **125 °C** | **225 °C** |
| POR-C12 | 1.20 | 0.32 |
| POR-C13 | 0.78 | 0.10 |
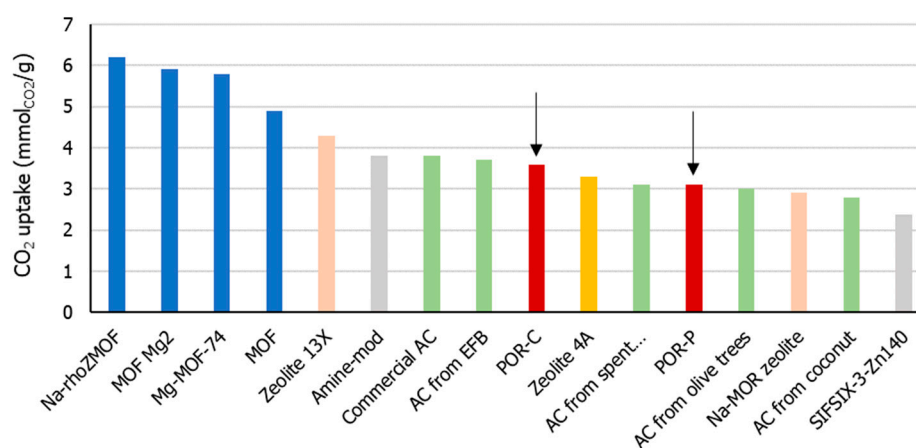


**Figure 7.** Carbon dioxide uptake for different adsorbent materials. Ref: Na-rhoZMOF [14,29], MOF $Mg_2$(dobdc) [30], Mg-MOF-74 [31], MOF $Mg_2$(dobdc)$(N_2H_4)$1.8 ($Mg_2$(dobdc)] (Amine-functionalized MOF H4dobdc = 2,5-dihydroxyl-1,4-benzenedicarboxylic acid) [29,32], Zeolite 13X [14,33], Amine-functionalized MOF $(Zn_2(C_2O_4)(C_2N_4H_3)_2$-$(H_2O)0.5)$ [34], Commercial AC [27], AC from EFB [35], Zeolite 4A [36], AC from spent coffee [14], AC from olive stones [37], Na-MOR zeolite [33], AC from coconut fibre [38], SIFSIX-3-Zn140 [29,39].

Finally, it is worth noting that, even though not carried out in this work, activated carbons can be completely regenerated (i.e., adsorption is reversible) due to the establishment of weak interactions between $CO_2$ molecules and the sorbent surface active sites [40]. This feature is highly desirable for potential industrial-scale applications and would help in promoting further circular economy strategies.

## 4. Conclusions

We have successfully activated biochars obtained from palm oil residues (empty fruit bunches and kernels), using physical and chemical processes. The resulting activated carbons are suitable for $CO_2$ adsorption, in equimolar mixtures with $N_2$, and show gas uptakes competitive to other existing carbonaceous materials. The utilisation of NaOH as a chemical activator increased the $CO_2$ adsorption, with respect to the physically activated materials, attributed to an increased selectivity towards $CO_2$ adsorption. The $CO_2$ adsorption capacity decreases with increasing temperature in accordance with the exothermicity of the process.

Our results suggest that the activated carbons obtained from oil palm residues can be used as efficient adsorbents for $CO_2$, with potential in carbon capture applications. Our experimental process can promote circular economy strategies by alleviating the accumulation of palm oil wastes. To close the cycle, the captured $CO_2$ could be re-used in the process of physical activation.

**Author Contributions:** B.A., S.F., A.M. and S.B.: validation, data curation and formal analysis; A.M.-F. and C.F.M.: conceptualisation, investigation, resources, writing—review and editing, funding

acquisition; C.M.: conceptualisation, methodology, writing—original draft preparation; F.H.: conceptualisation; E.A.: supervision. All authors have read and agreed to the published version of the manuscript.

**Data Availability Statement:** Not applicable.

**Conflicts of Interest:** The authors declare no conflict of interest.
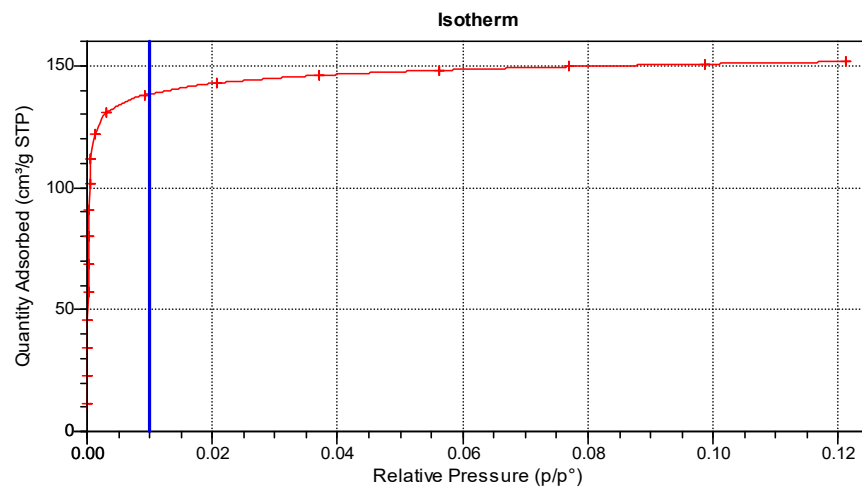
## Appendix A



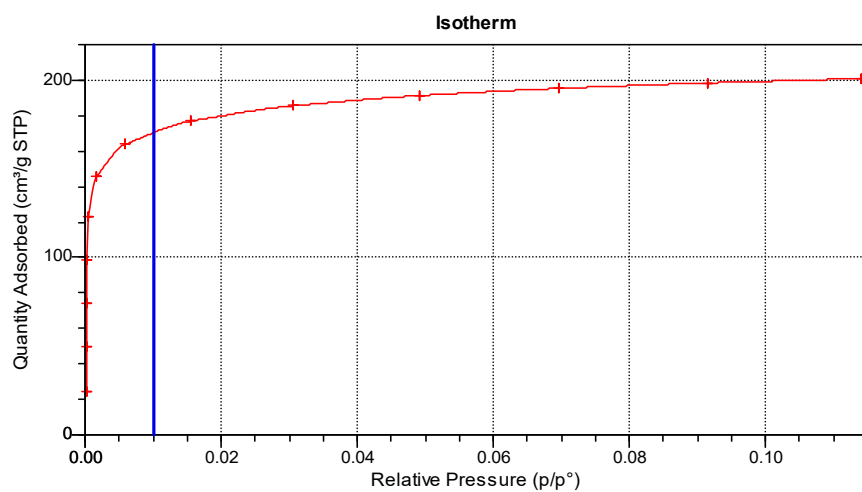**Figure A1.** BET isotherm POR-P20.


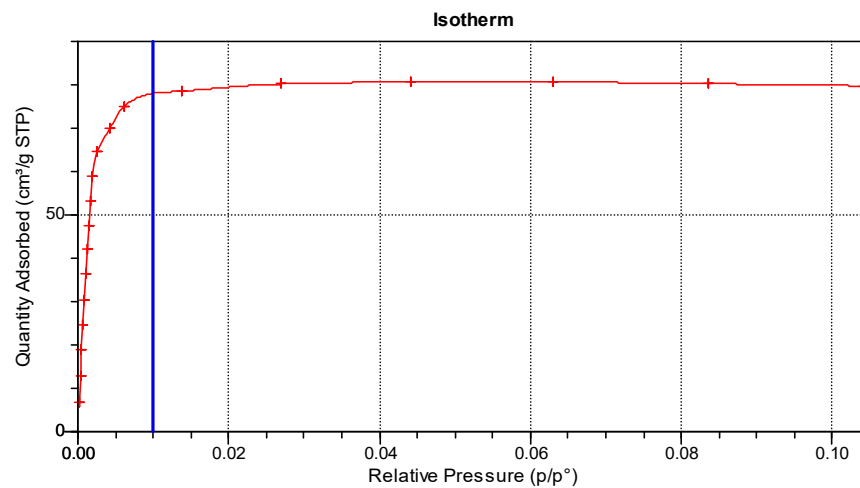
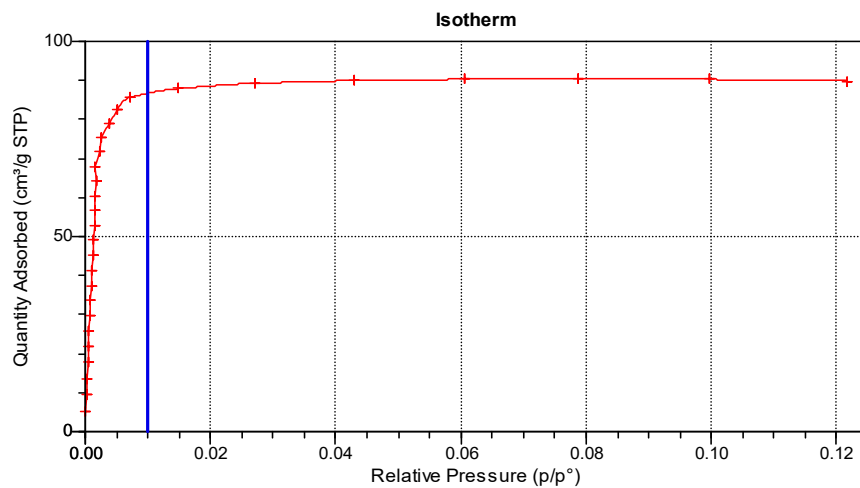**Figure A2.** BET isotherm POR-P40.

**Figure A3.** BET isotherm POR-C11.



**Figure A4.** BET isotherm POR-C12.

## References

1. FAOSTAT. Food and Agriculture Organisation of the United Nations. Available online: http://www.fao.org/home/en (accessed on 18 January 2022).
2. Zakaria, Z.; Rahim, A.R.A.; Aman, Z. Issues and Challenges of Oil Palm Cooperatives towards Greater Sustainability: A Proposal of Conceptual Framework. *Int. J. Acad. Res. Bus. Soc. Sci.* **2020**, *10*, 46–69. [CrossRef] [PubMed]
3. Zaki, H.H.M.; Rahim, M.A. *Palm Oil: Malaysia—EU Trade Issue*; Khazanah Research Institute: Kuala Lumpur, Malaysia, 2019.
4. Abdullah, N.; Sulaim, F. The Oil Palm Wastes in Malaysia. In *Biomass Now—Sustainable Growth and Use*; InTech: London, UK, 2013. [CrossRef]
5. Kaniapan, S.; Hassan, S.; Ya, H.; Nesan, K.P.; Azeem, M. The Utilisation of Palm Oil and Oil Palm Residues and the Related Challenges as a Sustainable Alternative in Biofuel, Bioenergy, and Transportation Sector: A Review. *Sustainability* **2021**, *13*, 3110. [CrossRef]
6. Pardakhti, M.; Jafari, T.; Tobin, Z.; Dutta, B.; Moharreri, E.; Shemshaki, N.S.; Suib, S.; Srivastava, R. Trends in Solid Adsorbent Materials Development for $CO_2$ Capture. *ACS Appl. Mater. Interfaces* **2019**, *11*, 34533–34559. [CrossRef]
7. Yahya, M.A.; Mansor, M.H.; Zolkarnaini, W.A.A.W.; Rusli, N.S.; Aminuddin, A.; Mohamad, K.; Sabhan, F.A.M.; Atik, A.A.A.; Ozair, L.N. *A Brief Review on Activated Carbon Derived from Agriculture By-Product*; AIP Publishing LLC: Melville, NY, USA, 2018; p. 030023. [CrossRef]
8. Serafin, J.; Narkiewicz, U.; Morawski, A.W.; Wróbel, R.J.; Michalkiewicz, B. Highly microporous activated carbons from biomass for $CO_2$ capture and effective micropores at different conditions. *J. $CO_2$ Util.* **2017**, *18*, 73–79. [CrossRef]
9. Deng, S.; Wei, H.; Chen, T.; Wang, B.; Huang, J.; Yu, G. Superior $CO_2$ adsorption on pine nut shell-derived activated carbons and the effective micropores at different temperatures. *Chem. Eng. J.* **2014**, *253*, 46–54. [CrossRef]
10. Ioannidou, O.; Zabaniotou, A. Agricultural residues as precursors for activated carbon production-A review. *Renew. Sustain. Energy Rev.* **2007**, *11*, 1966–2005. [CrossRef]

11. Sajjadi, B.; Chen, W.-Y.; Egiebor, N.O. A comprehensive review on physical activation of biochar for energy and environmental applications. *Rev. Chem. Eng.* **2019**, *35*, 735–776. [CrossRef]

12. Ukanwa, K.; Patchigolla, K.; Sakrabani, R.; Anthony, E.; Mandavgane, S. A Review of Chemicals to Produce Activated Carbon from Agricultural Waste Biomass. *Sustainability* **2019**, *11*, 6204. [CrossRef]

13. Hinkov, I.P.I.; Lamari, F.; Langlois, P.; Dicko, M.; Chilev, C. Carbon Dioxide Capture by Adsorption (review). *J. Chem. Technol. Metall. (JCTM)* **2016**, *51*, 609–626.

14. Ben-Mansour, R.; Habib, M.A.; Bamidele, O.E.; Basha, M.; Qasem, N.A.A.; Peedikakkal, A.; Laoui, T.; Ali, M.J.A.E. Carbon capture by physical adsorption: Materials, experimental investigations and numerical modeling and simulations—A review. *Appl. Energy* **2016**, *161*, 225–255. [CrossRef]

15. Promraksa, A.; Rakmak, N. Biochar production from palm oil mill residues and application of the biochar to adsorb carbon dioxide. *Heliyon* **2020**, *6*, e04019. [CrossRef] [PubMed]

16. Ibrahim, I.; Tsubota, T.; Hassan, M.A.; Andou, Y. Surface Functionalization of Biochar from Oil Palm Empty Fruit Bunch through Hydrothermal Process. *Processes* **2021**, *9*, 149. [CrossRef]

17. Lawal, A.A.; Hassan, M.A.; Farid, M.A.A.; Yasim-Anuar, T.A.T.; Yusoff, M.Z.M.; Zakaria, M.R.; Roslan, A.M.; Mokhtar, M.N.; Shirai, Y. Production of biochar from oil palm frond by steam pyrolysis for removal of residual contaminants in palm oil mill effluent final discharge. *J. Clean. Prod.* **2020**, *265*, 121643. [CrossRef]

18. Cristina, A.M.; Antonucci, B.; Focacci, S.; Heap, J.M.; Martel, A.M.; Hamzah, F.; Martín, C.F.; Martinez-Felipe, A. Molecular dynamics simulation of the interactions between carbon dioxide and a natural-based carbonaceous microporous material. *Chem. Eng. Trans.* **2021**, *86*, 1111–1116. [CrossRef]

19. Arami-Niya, A.; Daud, W.M.A.W.; Mjalli, F.S. Comparative study of the textural characteristics of oil palm shell activated carbon produced by chemical and physical activation for methane adsorption. *Chem. Eng. Res. Des.* **2011**, *89*, 657–664. [CrossRef]

20. Nuilerd, J.C.T.; Pongyeela, P. Pellet activated carbon production using parawood charcoal from gasifier by KOH activation for adsorption of iron in water. *Songklanakarin J. Sci. Technol.* **2018**, *40*, 264–270. [CrossRef]

21. Evans, M.J.B.; Halliop, E.; MacDonald, J.A.F. The production of chemically-activated carbon. *Carbon N. Y.* **1999**, *37*, 269–274. [CrossRef]

22. Correa, C.R.; Ngamying, C.; Klank, D.; Kruse, A. Investigation of the textural and adsorption properties of activated carbon from HTC and pyrolysis carbonizates. *Biomass Convers. Biorefinery* **2018**, *8*, 317–328. [CrossRef]

23. Li, W.; Yang, K.; Peng, J.; Zhang, L.; Guo, S.; Xia, H. Effects of carbonization temperatures on characteristics of porosity in coconut shell chars and activated carbons derived from carbonized coconut shell chars. *Ind. Crops Prod.* **2008**, *28*, 190–198. [CrossRef]

24. Parshetti, G.K.; Chowdhury, S.; Balasubramanian, R. Biomass derived low-cost microporous adsorbents for efficient $CO_2$ capture. *Fuel* **2015**, *148*, 246–254. [CrossRef]

25. Ello, A.S.; de Souza, L.K.C.; Trokourey, A.; Jaroniec, M. Development of microporous carbons for $CO_2$ capture by KOH activation of African palm shells. *J. $CO_2$ Util.* **2013**, *2*, 35–38. [CrossRef]

26. Rashidi, N.A.; Yusup, S. Production of palm kernel shell-based activated carbon by direct physical activation for carbon dioxide adsorption. *Environ. Sci. Pollut. Res.* **2019**, *26*, 33732–33746. [CrossRef] [PubMed]

27. Sulistianti, I.M.I.; Krisnandi, Y.K. Study of $CO_2$ adsorption capacity of mesoporous carbon and activated carbon modified by triethylenetetramine (TETA). *IOP Conf. Ser. Mater. Sci. Eng.* **2017**, *188*, 012041. [CrossRef]

28. Zhang, Z.; Zhou, J.; Xing, W.; Xue, Q.; Yan, Z.; Zhuo, S.; Qiao, S.Z. Critical role of small micropores in high $CO_2$ uptake. *Phys. Chem. Chem. Phys.* **2013**, *15*, 2523. [CrossRef]

29. Hu, Z.; Wang, Y.; Shah, B.B.; Zhao, D. CO2 Capture in Metal-Organic Framework Adsorbents: An Engineering Perspective. *Adv. Sustain. Syst.* **2019**, *3*, 1800080. [CrossRef]

30. Xiang, S.; He, Y.; Zhang, Z.; Wu, H.; Zhou, W.; Krishna, R.; Chen, B. Microporous metal-organic framework with potential for carbon dioxide capture at ambient conditions. *Nat. Commun.* **2012**, *3*, 954. [CrossRef]

31. Qasem, N.A.A.; Ben-Mansour, R. Adsorption breakthrough and cycling stability of carbon dioxide separation from $CO_2/N_2/H_2O$ mixture under ambient conditions using 13X and Mg-MOF-74. *Appl. Energy* **2018**, *230*, 1093–1107. [CrossRef]

32. Liao, P.Q.; Chen, X.W.; Liu, S.Y.; Li, X.Y.; Xu, Y.T.; Tang, M.; Rui, Z.; Ji, H.; Zhang, J.P.; Chen, X.M. Putting an ultrahigh concentration of amine groups into a metal–organic framework for $CO_2$ capture at low pressures. *Chem. Sci.* **2016**, *7*, 6528–6533. [CrossRef]

33. Villarreal, A.; Garbarino, G.; Riani, P.; Finocchio, E.; Bosio, B.; Ramirez, J.; Busca, G. Adsorption and separation of $CO_2$ from $N_2$-rich gas on zeolites: Na-X faujasite vs. Na-mordenite. *J. $CO_2$ Util.* **2017**, *19*, 266–275. [CrossRef]

34. Vaidhyanathan, R.; Iremonger, S.S.; Dawson, K.W.; Shimizu, G.K.H. An amine-functionalized metal organic framework for preferential CO2 adsorption at low pressures. *Chem. Commun.* **2009**, 5230. [CrossRef]

35. Yang, G.; Ye, J.; Yan, Y.; Tang, Z.; Yu, D.; Yang, J. Preparation and $CO_2$ adsorption properties of porous carbon from camphor leaves by hydrothermal carbonization and sequential potassium hydroxide activation. *RSC Adv.* **2017**, *7*, 4152–4160. [CrossRef]

36. Dreisbach, F.; Staudt, R.; Keller, J.U. High Pressure Adsorption Data of Methane, Nitrogen, Carbon Dioxide and their Binary and Ternary Mixtures on Activated Carbon. *Adsorption* **1999**, *5*, 215–227. [CrossRef]

37. González, A.S.; Plaza, M.G.; Rubiera, F.; Pevida, C. Sustainable biomass-based carbon adsorbents for post-combustion $CO_2$ capture. *Chem. Eng. J.* **2013**, *230*, 456–465. [CrossRef]

38. Hauchhum, L.; Mahanta, P. Carbon dioxide adsorption on zeolites and activated carbon by pressure swing adsorption in a fixed bed. *Int. J. Energy Environ. Eng.* **2014**, *5*, 349–356. [CrossRef]

39. Forrest, K.A.; Pham, T.; Elsaidi, S.K.; Mohamed, M.H.; Thallapally, P.K.; Zaworotko, M.J.; Space, B. Investigating $CO_2$ Sorption in SIFSIX-3-M (M = Fe, Co, Ni, Cu, Zn) through Computational Studies. *Cryst. Growth Des.* **2019**, *19*, 3732–3743. [CrossRef]

40. Choi, S.; Drese, J.H.; Jones, C.W. Adsorbent Materials for Carbon Dioxide Capture from Large Anthropogenic Point Sources. *ChemSusChem* **2009**, *2*, 796–854. [CrossRef]